

Consistent Second-Order Conic Integer Programming for Learning Bayesian Networks

Simge Küçükyavuz^{*†} Ali Shojaie^{† ‡} Hasan Manzour[§] Linchuan Wei[¶]

June 16, 2020

Abstract

Bayesian Networks (BNs) represent conditional probability relations among a set of random variables (nodes) in the form of a directed acyclic graph (DAG), and have found diverse applications in knowledge discovery. We study the problem of learning the sparse DAG structure of a BN from continuous observational data. The central problem can be modeled as a mixed-integer program with an objective function composed of a convex quadratic loss function and a regularization penalty subject to linear constraints. The optimal solution to this mathematical program is known to have desirable statistical properties under certain conditions. However, the state-of-the-art optimization solvers are not able to obtain provably optimal solutions to the existing mathematical formulations for medium-size problems within reasonable computational times. To address this difficulty, we tackle the problem from both computational and statistical perspectives. On the one hand, we propose a concrete early stopping criterion to terminate the branch-and-bound process in order to obtain a near-optimal solution to the mixed-integer program, and establish the consistency of this approximate solution. On the other hand, we improve the existing formulations by replacing the linear “big- M ” constraints that represent the relationship between the continuous and binary indicator variables with second-order conic constraints. Our numerical results demonstrate the effectiveness of the proposed approaches.

Keywords: Mixed-integer conic programming, Bayesian networks, directed acyclic graphs, early stopping criterion, consistency

1 Introduction

A Bayesian network (BN) is a probabilistic graphical model consisting of a labeled directed acyclic graph (DAG) $\mathcal{G} = (V, E)$, in which the vertex set $V = \{V_1, \dots, V_m\}$ corresponds to m random variables, and the edge set E prescribes a decomposition of the joint probability distribution of the random variables based on their parents in \mathcal{G} . The edge set E encodes Markov relations on

^{*}Department of Industrial Engineering and Management Sciences, Northwestern University (simge@northwestern.edu).

[†]These authors contributed equally to this work.

[‡]Department of Biostatistics, University of Washington (ashojaie@uw.edu).

[§]Department of Industrial and Systems Engineering, University of Washington (hmanzour@uw.edu).

[¶]Department of Industrial Engineering and Management Sciences, Northwestern University (Linchuan-Wei2022@u.northwestern.edu).

the nodes in the sense that each node is conditionally independent of its non-descendants given its parents. BNs have been used in knowledge discovery [47, 9], classification [1], feature selection [22], latent variable discovery [28] and genetics [35]. They also play a vital part in causal inference [37].

In this paper, we propose mixed-integer quadratic programming (MIQP) formulations for learning the optimal DAG structure of BNs given n continuous observations from a system of linear structural equation models (SEMs). While there exist exact integer-programming (IP) formulations for learning DAG structure with *discrete* data [11, 12, 26, 48, 4, 32, 33, 5, 13, 14], the development of tailored computational tools for learning the optimal DAG structure from *continuous* data has received less attention. In principle, exact methods developed for discrete data can be applied to continuous data. However, such methods result in exponentially sized formulations in terms of the number of binary variables. A common practice to circumvent the exponential number of binary variables is to limit the in-degree of each node [12, 14, 5]. But, this may result in sub-optimal solutions. On the contrary, MIQP formulations for learning DAGs corresponding to linear SEMs require a *polynomial* number of binary variables. This is because for BNs with linear SEMs, the score function — i.e., the penalized negative log-likelihood (PNL) — can be explicitly written as a function of the coefficients of linear SEMs [43, 50, 36, 30].

Continuous BNs with linear SEMs have witnessed a growing interest in the statistics and computer science communities [50, 40, 29, 23, 45]. In particular, it has been shown that the solution obtained from solving the PNL augmented by ℓ_0 regularization achieves desirable statistical properties [38, 50, 29]. Moreover, if the model is *identifiable* [38, 29], such a solution is guaranteed to uncover the true causal DAG when the sample size n is large enough. However, given the difficulty of obtaining exact solutions, existing approaches for learning DAGs from linear SEMs have primarily relied on *heuristics*, using techniques such as coordinate descent [21, 2, 25] and non-convex continuous optimization [56]. Unfortunately, these heuristics are not guaranteed to achieve the desirable properties of the global optimal solution. Moreover, it is difficult to evaluate the statistical properties of a sub-optimal solution with no optimality guarantees [27]. To bridge this gap, in this paper we develop mathematical formulations for learning optimal BNs from linear SEMs using a PNL objective with ℓ_0 regularization. By connecting the optimality gap of the mixed-integer program to the statistical properties of the solution, we also establish an *early stopping criterion* under which we can terminate the branch-and-bound procedure and attain a solution which asymptotically recovers the true parameters with high probability.

Our work is related to recent efforts to develop exact tailored methods for DAG learning from continuous data. [52] show that A^* -lasso algorithm tailored for DAG structure learning from continuous data with ℓ_1 -regularization is more effective than the previous approaches based on dynamic programming [e.g., 44] that are suitable for both discrete and continuous data. [36] develop a mathematical program for DAG structure learning with ℓ_1 regularization. [30] improve and extend the formulation by [36] for DAG learning from continuous data with both ℓ_0 and ℓ_1 regularizations. The numerical experiments by [30] demonstrate that as the number of nodes grows, their MIQP formulation outperforms A^* -lasso and the existing IP methods; this improvement is both in terms of reducing the IP optimality gap, when the algorithm is stopped due to a time limit, and in terms of computational time, when the instances can be solved to optimality. In light of these recent efforts, the current paper makes important contributions to this problem at the intersection of statistics and optimization.

- The statistical properties of *optimal* PNL with ℓ_0 regularization have been studied extensively [29, 50]. However, it is often difficult to obtain an optimal solution and no results have been established on the statistical properties of approximate solutions. In this pa-

per, we give an early stopping criterion for the branch-and-bound process under which the approximate solution gives consistent estimates of the true coefficients of the linear SEM. Our result leverages the statistical consistency of the PNL estimate with ℓ_0 regularization [50, 38] along with the properties of the branch-and-bound method wherein both lower and upper bound values on the objective function are available at each iteration. By connecting these two properties, we obtain a concrete early stopping criterion, as well as a simple proof of consistency of the approximate solution. To the best of our knowledge, this result is the first of its kind for DAG learning.

- In spite of recent progress, a key challenge in learning DAGs from linear SEMs is enforcing bounds on arc weights. This is commonly modeled using the standard “big- M constraint” approach [36, 30]. As shown by [30], this strategy leads to poor continuous relaxations for the problem, which in turn results in slow lower bound improvement in the branch-and-bound tree. In particular, [30] establish that all existing big- M formulations achieve the same continuous relaxation objective function under a mild condition (see Proposition 4). To circumvent this issue, we present a mixed-integer second-order cone program (MISOCP), which gives a tighter continuous relaxation than existing big- M formulations. This formulation can be solved by powerful state-of-the-art optimization packages. Our numerical results show the superior performance of MISOCP compared to the existing big- M formulations in terms of improving the lower bound and reducing the optimality gap.

The rest of the paper is organized as follows. In Section 2, we define the DAG structure learning problem corresponding to linear SEMs, and give a general framework for the problem. In Section 3, we present our early stopping criterion and establish the asymptotic properties of the solution obtained under this stopping rule. We review existing mathematical formulations in Section 4, and present our proposed mathematical formulations in Section 5. Results of comprehensive numerical studies are presented in Section 6. We end the paper with a summary in Section 7.

2 Problem setup: Penalized DAG estimation with linear SEMs

Let $\mathcal{M} = (V, E)$ be an undirected and possibly cyclic super-structure graph with node set $V = \{1, 2, \dots, m\}$ and edge set $E \subseteq V \times V$; let $\vec{\mathcal{M}} = (V, \vec{E})$ be the corresponding bi-directional graph with $\vec{E} = \{(j, k), (k, j) | (j, k) \in E\}$. We refer to undirected edges as *edges* and directed edges as *arcs*.

We assume that causal effects of continuous random variables in a DAG \mathcal{G}_0 are represented by m linear regressions of the form

$$X_k = \sum_{j \in pa_k^{\mathcal{G}_0}} \beta_{jk} X_j + \epsilon_k, \quad k = 1, \dots, m, \quad (1)$$

where X_k is the random variable associated with node k , $pa_k^{\mathcal{G}_0}$ represents the parents of node k in \mathcal{G}_0 , i.e., the set of nodes with arcs pointing to k ; the latent random variable ϵ_k denotes the unexplained variation in node k ; and BN parameter β_{jk} specifies the effect of node j on k for $j \in pa_k^{\mathcal{G}_0}$. The above model is known as a linear SEM [37].

Let $\mathcal{X} = (\mathcal{X}_1, \dots, \mathcal{X}_m)$ be the $n \times m$ data matrix with n rows representing i.i.d. samples from each random variable, and m columns representing random variables X_1, \dots, X_m . The linear SEM (1) can be compactly written in matrix form as $\mathcal{X} = \mathcal{X}B + \mathcal{E}$, where $B = [\beta] \in \mathbb{R}^{m \times m}$ is a matrix with $\beta_{kk} = 0$ for $k = 1, \dots, m$, $\beta_{jk} = 0$ for all $(j, k) \notin E$, and \mathcal{E} is the $n \times m$ ‘noise’ matrix. Then, $\mathcal{G}(B)$ denotes the directed graph on m nodes such that arc (j, k) appears in $\mathcal{G}(B)$ if and only if $\beta_{jk} \neq 0$. Throughout the paper, we will use B and β to denote the matrix of coefficients and its vectorized version.

A key challenge when estimating DAGs by minimizing the loss function (2) is that the true DAG is generally not identifiable from observational data. However, for certain SEM distributions, the true DAG is in fact identifiable from observational data. Two important examples are linear SEMs with possibly non-Gaussian homoscedastic noise variables [38], as well as linear SEMs with unequal noise variances that are known up to a constant [29]. In these special cases, the true DAG can be identified from observational data, without requiring the (strong) ‘faithfulness’ assumption, which is known to be restrictive in high dimensions [49, 46]. Given these important implications, in this paper we focus on learning Bayesian networks corresponding to the above *identifiable* linear SEMs.

The negative log likelihood for an identifiable linear SEM (1) with equal noise variances is proportional to

$$l(\beta; \mathcal{X}) = n \operatorname{tr} \left\{ (I - B)(I - B)^\top \widehat{\Sigma} \right\}; \quad (2)$$

here $\widehat{\Sigma} = n^{-1} \mathcal{X}^\top \mathcal{X}$ is the empirical covariance matrix, and I is the identity matrix [43, 50].

To learn *sparse* DAGs, van de Geer and Bühlmann [50] propose to augment the negative log likelihood with an ℓ_0 regularization term. Given a super-structure \mathcal{M} , the optimization problem corresponding to this penalized negative log-likelihood (PNLM) is given by

$$\text{PNLM} \quad \min_{B \in \mathbb{R}^{m \times m}} \mathcal{L}(\beta) := l(\beta; \mathcal{X}) + \lambda_n \|\beta\|_0 \quad (3a)$$

$$\text{s.t. } \mathcal{G}(B) \text{ induces a DAG from } \overline{\mathcal{M}}, \quad (3b)$$

where the tuning parameter λ_n controls the degree of the ℓ_0 regularization, and the constraint (3b) stipulates that the resulting directed subgraph is a DAG induced from $\overline{\mathcal{M}}$. When \mathcal{M} corresponds to a complete graph, PNL \mathcal{M} reduces to the original PNL of van de Geer and Bühlmann [50].

The choice of ℓ_0 regularization in (3) is deliberate. Although ℓ_1 regularization has attractive computational and statistical properties in high-dimensional regression [8], many of these advantages disappear in the context of DAG structure learning [21, 2]. By considering ℓ_0 regularization, [50] establish the consistency of PNL under appropriate assumptions. More specifically, for a Gaussian SEM, they show that the estimated DAG has (asymptotically) the same number of edges as the DAG with minimal number of edges (minimal-edge I-MAP), and establish the consistency of PNL for learning sparse DAGs. These results are formally stated in Proposition 1 in the next section.

Remark 1. A Tikhonov (ℓ_2) regularization term, $\mu \|\beta\|_2^2$, for a given $\mu > 0$, can also be added to the objective (3a) to obtain more stable solutions [7].

In our earlier work [30], we observe that existing mathematical formulations are slow to converge to a provably optimal solution, β^* , of (3) using the state-of-the-art optimization solvers. Therefore, the solution process needs to be terminated early to yield a feasible solution, $\hat{\beta}$ with a positive optimality gap, i.e., a positive difference between the upper bound on $\mathcal{L}(\beta^*)$ provided by $\mathcal{L}(\hat{\beta})$ and a lower bound on $\mathcal{L}(\beta^*)$ provided by the best continuous relaxation obtained by the branch-and-bound

algorithm upon termination. However, statistical properties of such a sub-optimal solution are not well-understood. Therefore, there exists a gap between theory and computation: while the optimal solution has nice statistical properties, the properties of the solutions obtained from approximate computational algorithms are not known. Moreover, due to the non-convex and complex nature of the problem, characterizing the properties of the solutions provided by heuristics is especially challenging. In the next section, we bridge this gap by developing a concrete early stopping criterion and establishing the consistency of the solution obtained using this criterion.

3 Early stopping criterion for DAG learning

In this section, we establish a sufficient condition for the approximate solution of PNL \mathcal{M} , $\hat{\beta}$ to be consistent for the true coefficients, β^0 ; that is $\|\beta^0 - \hat{\beta}\|_2^2 = \mathcal{O}(s^0 \log(m)/n)$, where s^0 is the number of arcs in the true DAG, and $x \asymp y$ means that x converges to y asymptotically. This result is obtained by leveraging an important property of the branch-and-bound process for integer programming that provides both lower and upper bounds on the objective function $\mathcal{L}(\beta^*)$ upon early stopping, as well as the consistency results of the PNL estimate with ℓ_0 regularization. Using the insight from this new result, we then propose a concrete stopping criterion for terminating the branch-and-bound process that results in consistent parameter estimates.

Let LB and UB respectively denote the lower and upper bounds on the optimal objective function value (3a) obtained from solving (3) under an early stopping criterion (i.e., when the obtained solution is not necessarily optimal). We define the difference between the upper and lower bounds as the *absolute* optimality gap: $GAP = UB - LB$. Let $\hat{\mathcal{G}}$ and $\hat{\beta}$ denote the structure of the DAG and coefficients of the arcs from optimization model (3) under the early stopping condition with sample size n and regularization parameter λ_n . Let \mathcal{G}^* and β^* denote the DAG structure and coefficients of arcs obtained from the optimal solution of (3), and \mathcal{G}^0 and β^0 denote the true DAG structure and the coefficient of arcs, respectively. We denote the number of arcs in $\hat{\mathcal{G}}$, \mathcal{G}^0 , and \mathcal{G}^* by \hat{s} , s^0 , and s^* , respectively. The score value in (3a) of each solution is denoted by $\mathcal{L}(\phi)$ where $\phi \in \{\beta^*, \hat{\beta}, \beta^0\}$.

Next, we present our main result. Our result extends van de Geer and Bühlmann’s result on consistency of PNL \mathcal{M} for the optimal, but computationally unattainable, estimator, β^* to an approximate estimator, $\hat{\beta}$, obtained from early stopping. In the following (including the statement of our main result, Proposition 2), we assume that the super-structure \mathcal{M} is known *a priori*. The setting where \mathcal{M} is estimated from data is discussed at the end of the section. We begin by stating the key result from [50] and the required assumptions. Throughout, we consider a Gaussian linear SEM of the form (1). We denote the variance of error terms, ϵ_j , by σ_{jj}^2 and the true covariance matrix of the set of random variables, (X_1, \dots, X_m) by the $m \times m$ matrix Σ .

Assumption 1. For some constant σ_0^2 , it holds that $\max_{j=1, \dots, m} \sigma_{jj}^2 \leq \sigma_0^2$. Moreover, the smallest eigenvalue of Σ , $\kappa_{\min}(\Sigma)$, is nonzero.

Assumption 2. Let, as in [50], $\tilde{\Omega}(\pi)$ be the precision matrix of the vector of noise variables for an SEM given permutation π of nodes. Denoting the diagonal entries of this matrix by $\tilde{\omega}_{jj}$, there exists a constant $\omega_0 > 0$ such that if $\tilde{\Omega}(\pi)$ is not a multiple of the identity matrix, then

$$m^{-1} \sum_{j=1}^m ((\tilde{\omega}_{jj})^2 - 1)^2 > 1/\omega_0.$$

Proposition 1. (Theorem 5.1 in [50]) Suppose Assumptions 1 and 2 hold. Let $\alpha_0 := \min\{\frac{4}{m}, 0.05\}$. Then for an ℓ_0 regularization parameter $\lambda \asymp \log(m)/n$, it holds with probability at least $1 - \alpha_0$ that

$$\|\beta^* - \beta^0\|_2^2 + \lambda s^* = \mathcal{O}(\lambda s^0).$$

Here, $\lambda = \lambda_n/n$, because the loss function (2) is that of [50] scaled by the sample size n . Before presenting our main result, we state one more condition on the covariance matrix of the random variables generated by linear SEM. For a given subset $S \subset \{1, \dots, m\}$, let S^c denote its complement, i.e., $S^c := \{1, \dots, m\} \setminus S$.

Definition [41]. Define the set $\mathcal{C}(S; \eta) := \{v \in \mathbb{R}^m \mid \|v_{S^c}\|_1 \leq \eta \|v_S\|_1\}$ for a given subset $S \subset \{1, \dots, m\}$ and constant $\eta \geq 1$. The $m \times m$ sample covariance matrix $\widehat{\Sigma} = n^{-1} \mathcal{X}^\top \mathcal{X}$ satisfies the *restricted eigenvalue (RE) condition over S* with parameters $(\eta, \gamma) \in [1, \infty) \times [0, \infty)$ if

$$\frac{1}{n} v^\top \mathcal{X}^\top \mathcal{X} v = \frac{1}{n} \|\mathcal{X}v\|_2^2 \geq \gamma^2 \|v\|_2^2, \quad \forall v \in \mathcal{C}(S; \eta).$$

If this condition holds for all subsets S with cardinality s , we say that $\widehat{\Sigma}$ satisfies a *restricted eigenvalue (RE) condition of order s* with parameters (η, γ) . The $m \times m$ population covariance matrix Σ is said to satisfy the RE condition if

$$\|\Sigma^{1/2}v\|_2 \geq \gamma \|v\|_2 \quad \forall v \in \mathcal{C}(S; \eta).$$

Raskutti et al. [41] show that if Σ satisfies the RE condition, then there exists constants c and c' such that with probability at least $1 - c'e^{-cn}$, $\widehat{\Sigma}$ also satisfies the RE condition with parameters $(\eta, \gamma/8)$. More specifically, their proof of Corollary 1 shows that for any $v \in \mathcal{C}(S; \eta)$,

$$\|v\|_2^2 \leq c_1 \|\mathcal{X}v\|_2^2, \tag{4}$$

where $c_1 = n^{-1} \left\{ \frac{\gamma}{4} - 9(1 + \alpha)\sigma_0 \sqrt{\frac{s^0 \log(m)}{n}} \right\}^{-2}$ for σ_0 defined in Assumption 1. In fact, in the low-dimensional setting implied by condition (5), the inequality (4) holds with probability one because, when $m \ll n$, for any $v \in \mathbb{R}^m$ we have $\|\mathcal{X}v\|_2^2 \geq \kappa_{\min}(\mathcal{X}) \|v\|_2^2$. Thus, (4) holds with $c_1 = 1/\kappa_{\min}(\mathcal{X})$.

Proposition 2. Suppose Σ satisfies the RE condition of order s^0 with parameters (η, γ) and that for constants $c_2, c_3 > 0$,

$$n > \max \left\{ c_2 \frac{\sigma_0^2 (1 + \eta)^2}{\gamma^2} s^0 \log(m), c_3 m \log(n) \right\}. \tag{5}$$

Suppose also that Assumptions 1 and 2 hold. Let $\alpha_0 = \min\{\frac{4}{m}, 0.05\}$ and $\lambda \asymp \log(m)/n$. Then, the estimator $\hat{\beta}$ obtained from early stopping of the branch-and-bound process such that $GAP \asymp \mathcal{O}\left(\frac{\log(m)}{n} s^0\right)$ satisfies $\|\hat{\beta} - \beta^0\|_2^2 \asymp \mathcal{O}\left(\frac{\log(m)}{n} s^0\right)$ with probability $\min\{1 - \alpha_0, 1 - c'e^{-cn}\}$ for constants c and c' used for the RE condition.

Proof. First, by the triangle inequality and the fact that $2ab \leq a^2 + b^2, \forall a, b \in \mathbb{R}$,

$$\|\hat{\beta} - \beta^0\|_2^2 \leq 2\|\hat{\beta} - \beta^*\|_2^2 + 2\|\beta^* - \beta^0\|_2^2. \tag{6}$$

Further, by the sparsity of β^* from Proposition 1, $\hat{\beta} - \beta^*$ belongs to the set $\mathcal{C}(S^0; \eta)$, where $S^0 = \{j : \beta_j^0 \neq 0\}$ and $|S^0| = s^0$. Thus,

$$\|\hat{\beta} - \beta^*\|_2^2 \leq c_1 \|\mathcal{X}(\hat{\beta} - \beta^*)\|_2^2. \quad (7)$$

Now, noting that $\ell(\beta; \mathcal{X}) = \|\mathcal{X} - \mathcal{X}\beta\|_2^2$ (see, e.g., the expanded version in Eq. (10a)), we can write a Taylor series expansion of $\ell(\hat{\beta}; \mathcal{X})$ around $\ell(\beta^*; \mathcal{X})$ to get

$$\|\mathcal{X}(\hat{\beta} - \beta^*)\|_2^2 = \ell(\hat{\beta}; \mathcal{X}) - \ell(\beta^*; \mathcal{X}) - 2(\hat{\beta} - \beta^*)^\top \mathcal{X}^\top \mathcal{X}(\beta^* - \beta^0) + 2(\hat{\beta} - \beta^*)^\top \mathcal{X}^\top \mathcal{E}.$$

Here, we also use the fact that $\mathcal{X} = \mathcal{X}B^0 + \mathcal{E}$. Thus, using triangle inequality again, we get

$$\begin{aligned} \|\hat{\beta} - \beta^*\|_2^2 &\leq \\ c_1 \left| \ell(\hat{\beta}; \mathcal{X}) - \ell(\beta^*; \mathcal{X}) \right| &+ 2c_1 \kappa_{\max}(\mathcal{X}^\top \mathcal{X}) \|\hat{\beta} - \beta^*\|_2 \|\beta^* - \beta^0\|_2 + 2c_1 \|\hat{\beta} - \beta^*\|_2 \|\mathcal{X}^\top \mathcal{E}\|_2, \end{aligned}$$

where κ_{\max} denotes the maximum eigenvalue of the matrix. Let $Z = \|\hat{\beta} - \beta^*\|_2$, and denote $\Pi = 2c_1 [\kappa_{\max}(\mathcal{X}^\top \mathcal{X}) \|\beta^* - \beta^0\|_2 + \|\mathcal{X}^\top \mathcal{E}\|_2]$, and $\Gamma = c_1 \left| \ell(\hat{\beta}; \mathcal{X}) - \ell(\beta^*; \mathcal{X}) \right|$. Then, the above inequality can be written as $Z^2 \leq \Pi Z + \Gamma$, which implies that $Z \leq (\Pi + \sqrt{\Pi^2 + 4\Gamma})/2$. Let \mathcal{T} be the event under which $\Pi = o(1)$. Then, on the set \mathcal{T} ,

$$\|\hat{\beta} - \beta^*\|_2^2 \leq c_1 \left| \ell(\hat{\beta}; \mathcal{X}) - \ell(\beta^*; \mathcal{X}) \right| + o(1). \quad (8)$$

Plugging in (8) into (6), on the set \mathcal{T} we get

$$\begin{aligned} \|\hat{\beta} - \beta^0\|_2^2 &\leq 2c_1 \left| \ell(\hat{\beta}; \mathcal{X}) - \ell(\beta^*; \mathcal{X}) \right| + 2\|\beta^* - \beta^0\|_2^2 + o(1) \\ &\leq 2c_1 \left| \ell(\hat{\beta}; \mathcal{X}) - \ell(\beta^*; \mathcal{X}) + \lambda \hat{s} - \lambda s^* \right| + 2\|\beta^* - \beta^0\|_2^2 + 2c_1 |\lambda s^* - \lambda \hat{s}| + o(1) \\ &\leq 2c_1 \underbrace{\left| \ell(\hat{\beta}; \mathcal{X}) - \ell(\beta^*; \mathcal{X}) + \lambda \hat{s} - \lambda s^* \right|}_{\mathcal{L}(\hat{\beta}) - \mathcal{L}(\beta^*)} + 2\|\beta^* - \beta^0\|_2^2 + 2c_1 \lambda s^* + o(1) \\ &\leq 2c_1 GAP + 2(\|\beta^* - \beta^0\|_2^2 + c_1 \lambda s^*) + o(1), \end{aligned} \quad (9)$$

where the last inequality follows from the fact that, by definition, $\left| \mathcal{L}(\hat{\beta}) - \mathcal{L}(\beta^*) \right| \leq GAP$.

Now, by Proposition 1, we know that with probability at least $1 - \alpha_0$, $\|\beta^* - \beta^0\|_2^2 = \mathcal{O}(s^0 \log(m)/n)$, and $c_1 \lambda s^* = \mathcal{O}(c_1 s^0 \log(m)/n)$. Moreover, by the RE condition, with probability at least $1 - c'e^{-cn}$, $c_1 = \mathcal{O}(1)$. Finally, using concentration inequalities for the Gaussian SEM noise \mathcal{E} [e.g. 8], the probability of the set \mathcal{T} is lower bounded by the probability that $\|\beta^* - \beta^0\|_2^2 = \mathcal{O}(s^0 \log(m)/n)$, which is $1 - \alpha_0$. Thus, stopping the branch-and-bound algorithm when $GAP = \mathcal{O}(\lambda s^0)$ guarantees that, with probability at least $\min\{1 - \alpha_0, 1 - c'e^{-cn}\}$, $\|\hat{\beta} - \beta^0\|_2^2 = \mathcal{O}(s^0 \log(m)/n)$. \square

Proposition 2 suggests that the algorithm can be stopped by setting a threshold $c^* \lambda s^0$ on the value of $GAP = |UB - LB|$ for a constant $c^* > 0$, say $c^* = 1$. Such a solution will then achieve the same desirable statistical properties as the optimal solution β^* . However, while λ can be chosen data-adaptively (as discussed in Section 6), the value for s^0 is not known. However, one can find

an upper bound for s^0 based on the number of edges in the super-structure \mathcal{M} . In particular, if \mathcal{M} is the moral graph [37] with s_m edges, then $s^0 \leq s_m$. Thus, in this case, a consistent parameter estimate can be obtained if the branch-and-bound process is stopped when $GAP \leq s_m \lambda$.

The above results, including the specific choice of early stopping criterion, are also valid if the super-structure \mathcal{M} corresponding to the moral graph is not known *a priori*. That is because the moral graph can be consistently estimated from data using recent developments in graphical modeling; see Drton and Maathuis [16] for a review of the literature. While some of the existing algorithms based on ℓ_1 -penalty require an additional *irrepresentability* condition [31, 42], this assumption can be relaxed by using instead an adaptive lasso penalty or by thresholding the initial lasso estimates [8].

In light of Proposition 2, it is of great interest to develop algorithms that converge to a solution with a small optimality gap expeditiously. To achieve this, one approach is to obtain better lower bounds using the branch-and-bound process from strong mathematical formulations for (3). To this end, we next review existing formulations of (3).

4 Existing Formulations of DAG Learning with Linear SEMs

In this section, we review known mathematical formulations for DAG learning with linear SEMs. We first outline the necessary notation below.

Index Sets

$V = \{1, 2, \dots, m\}$: index set of random variables;

$\mathcal{D} = \{1, 2, \dots, n\}$: index set of samples.

Input

$\mathcal{M} = (V, E)$: an undirected super-structure graph (e.g., the moral graph);

$\vec{\mathcal{M}} = (V, \vec{E})$: the bi-directional graph corresponding to the undirected graph \mathcal{M} ;

$\mathcal{X} = (\mathcal{X}_1, \dots, \mathcal{X}_m)$, where $\mathcal{X}_v = (x_{1v}, x_{2v}, \dots, x_{nv})^\top$ and x_{dv} denotes d th sample ($d \in \mathcal{D}$) of random variable X_v ; note $\mathcal{X} \in \mathbb{R}^{n \times m}$;

λ_n : tuning parameter (penalty coefficient for ℓ_0 regularization).

Continuous optimization variables

β_{jk} : weight of arc (j, k) representing the regression coefficients $\forall (j, k) \in \vec{E}$.

Binary optimization variables

$z_{jk} = 1$ if arc (j, k) exists in a DAG; otherwise 0, $\forall (j, k) \in \vec{E}$,

$g_{jk} = 1$ if $\beta_{jk} \neq 0$; otherwise 0, $\forall (j, k) \in \vec{E}$.

Let $F(\beta, g) = \sum_{k \in V} \sum_{d \in \mathcal{D}} \left(x_{dk} - \sum_{(j,k) \in \vec{E}} \beta_{jk} x_{dj} \right)^2 + \lambda_n \sum_{(j,k) \in \vec{E}} g_{jk}$. The PNL \mathcal{M} can be

cast as the following optimization problem:

$$\min F(\beta, g), \quad (10a)$$

$$\mathcal{G}(B) \text{ induces a DAG from } \vec{\mathcal{M}}, \quad (10b)$$

$$\beta_{jk}(1 - g_{jk}) = 0, \quad \forall (j, k) \in \vec{E}, \quad (10c)$$

$$g_{jk} \in \{0, 1\}, \quad \forall (j, k) \in \vec{E}. \quad (10d)$$

The objective function (10a) is an expanded version of $\mathcal{L}(\beta)$ in PNL \mathcal{M} , where we use the indicator variable g_{jk} to encode the ℓ_0 regularization. The constraints in (10b) rule out cycles. The constraints in (10c) are non-linear and stipulate that $\beta_{jk} \neq 0$ only if $g_{jk} = 1$.

There are two sources of difficulty in solving (10a)-(10d): (i) the acyclic nature of DAG imposed by the combinatorial constraints in (10b); (ii) the set of *nonlinear* constraints in (10c), which stipulates that $\beta_{jk} \neq 0$ only if there exists an arc (j, k) in $\mathcal{G}(B)$. In Section 4.1, we discuss related studies to address the former, whereas in Section 4.2 we present relevant literature for the latter.

4.1 Linear encodings of the acyclicity constraints (10b)

There are several ways to ensure that the estimated graph does not contain any cycles. The first approach is to add a constraint for each cycle in the graph, so that at least one arc in this cycle must not exist in $\mathcal{G}(B)$. A *cutting plane* (CP) method is used to solve such a formulation which may require generating an exponential number of constraints. Another way to rule out cycles is by imposing constraints such that the nodes follow a topological order [36]. A topological ordering is a unique ordering of the nodes of a graph from 1 to m such that the graph contains an arc (j, k) if node j appears before node k in the order. We refer to this formulation as *topological ordering* (TO). The *layered network* (LN) formulation proposed by [30] improves the TO formulation by reducing the number of binary variables. [30] discuss these formulations in detail.

Let \mathcal{C} be the set of all possible directed cycles and $\mathcal{C}_A \in \mathcal{C}$ be the set of arcs defining a cycle. The CP formulation removes cycles by imposing the following constraints for (10b)

$$\text{CP} \quad \sum_{(j,k) \in \mathcal{C}_A} g_{jk} \leq |\mathcal{C}_A| - 1, \quad \forall \mathcal{C}_A \in \mathcal{C}. \quad (11)$$

Define decision variables $z_{jk} \in \{0, 1\}$ for all $(j, k) \in \vec{E}$ and $o_{rs} \in \{0, 1\}$ for all $r, s \in \{1, \dots, m\}$. The variable z_{jk} takes value 1 if there is an arc (j, k) in the network, and o_{rs} takes value 1 if the topological order of node r equals s . The TO formulation rules out cycles in the graph by the following constraints

$$\text{TO} \quad g_{jk} \leq z_{jk}, \quad \forall (j, k) \in \vec{E}, \quad (12a)$$

$$z_{jk} - mz_{kj} \leq \sum_{s \in V} s(o_{ks} - o_{js}), \quad \forall (j, k) \in \vec{E}, \quad (12b)$$

$$\sum_{s \in V} o_{rs} = 1 \quad \forall r \in V, \quad (12c)$$

$$\sum_{r \in V} o_{rs} = 1 \quad \forall s \in V. \quad (12d)$$

The third way to remove cycles is by imposing the condition that the resulting graph is a layered network. This can be achieved by the following set of constraints in the LN formulation:

$$\text{LN} \quad g_{jk} \leq z_{jk} \quad \forall (j, k) \in \vec{E}, \quad (13a)$$

$$z_{jk} - (m - 1)z_{kj} \leq \psi_k - \psi_j \quad \forall (j, k) \in \vec{E}. \quad (13b)$$

Let ψ_k be the *layer value* for node k . The set of constraints in (13b) ensures that if the layer of node j appears before that of node k (i.e., there is a direct path from node j to node k), then $\psi_k \geq \psi_j + 1$. This rules out any cycles.

The set of constraints in (13b) imposes that if $z_{ij} = 1$ and $z_{jk} = 1$, then $z_{ik} = 1$. Thus, additional binary vector g along with the set of constraints in (13a) is needed to correctly encode the ℓ_0 regularization. Similar reasoning applies for the TO formulation; see [30].

4.2 Linear encodings of the non-convex constraints (10c)

The nonconvexity of the set of constraints in (10c) causes challenges in obtaining provably optimal solutions with existing optimization software. Therefore, we consider convex representations of this set of constraints. First, we consider a linear representation of the constraints in (10c). Although the existing formulations discussed in Section 4.1 differ in their approach to ruling out cycles, one major commonality among them is that they replace the non-linear constraint (10c) by so called *big- M constraints* given by

$$-Mg_{jk} \leq \beta_{jk} \leq Mg_{jk}, \forall (j, k) \in \vec{E}, \quad (14)$$

for a large enough M . Unfortunately, these big- M constraints (14) are poor approximations of (10c), especially in this problem, because no natural and tight value for M exist. Although a few techniques have been proposed for obtaining the big- M parameter for sparse regression problem [6, 24], the resulting parameters are often too large in practice. Further, finding a tight big- M parameter itself is a difficult problem to solve for DAG structure learning.

Consider (10a)-(10d) by substituting (10c) by the linear big- M constraints (14) and writing the objective function in a matrix form. We denote the resulting formulation, which has a convex quadratic objective and linear constraints, by the following MIQP.

$$\text{MIQP} \quad \min \quad \text{tr} [(I - B)(I - B)^\top \mathcal{X}^\top \mathcal{X}] + \lambda_n \sum_{(j,k) \in \vec{E}} g_{jk} \quad (15a)$$

$$(10b), (14) \quad (15b)$$

$$g_{jk} \in \{0, 1\} \quad \forall (j, k) \in \vec{E}. \quad (15c)$$

Depending on which types of constraints are used in lieu of (10b), as explained in Section 4.1, MIQP (16) results in three different formulations: MIQP+CP, which uses (11), MIQP+TO, which uses (12), and MIQP+LN, which uses (13), respectively.

To discuss the challenges of the big- M approach, we give a definition followed by two propositions.

Definition 1. A formulation A is said to be *stronger* than formulation B if $\mathcal{R}(A) \subset \mathcal{R}(B)$ where $\mathcal{R}(A)$ and $\mathcal{R}(B)$ correspond to the feasible regions of continuous relaxations of A and B , respectively.

Proposition 3. (Proposition 3 in [30]) *The MIQP+TO and MIQP+CP formulations are stronger than the MIQP+LN formulation.*

Proposition 4. (Proposition 5 in [30]) *Let β_{jk}^* denote the optimal coefficient associated with an arc $(j, k) \in \vec{E}$ from problem (3). For the same variable branching in the branch-and-bound process, the continuous relaxations of the MIQP+LN formulation for ℓ_0 regularizations attain the same optimal objective function value as MIQP+TO and MIQP+CP, if $M \geq 2 \max_{(j,k) \in \vec{E}} |\beta_{jk}^*|$.*

Proposition 3 implies that the MIQP+TO and MIQP+CP formulations are stronger than the MIQP+LN formulation. Nonetheless, Proposition 4 establishes that for sufficiently large values of M , stronger formulations attain the same continuous relaxation objective function value as the weaker formulation throughout the branch-and-bound tree. The optimal solution to the continuous relaxation of MIQP formulations of DAG structure learning may not be at an extreme point of the convex hull of feasible points. Hence, stronger formulations do not necessarily ensure better lower bounds. This is in contrast to a mixed-integer program (MIP) with linear objective, whose continuous relaxation is a linear program (LP). In that case, there exists an optimal solution that is an extreme point of the corresponding feasible set. As a result, a better lower bound can be obtained from a stronger formulation that better approximates the convex hull of a mixed-integer linear program; this generally leads to faster convergence. A prime example is the traveling salesman problem (TSP), for which stronger formulations attain better computational performance [34]. In contrast, the numerical results by [30] show that MIQP+LN has better computational performance because it is a compact formulation with the fewest constraints and the same continuous relaxation bounds.

Our next result, which is adapted from [15] to the DAG structure learning problem, shows that the continuous relaxation of MIQP is equivalent to the optimal solution to the problem where the ℓ_0 -regularization term is replaced with an ℓ_1 -regularization term (i.e., $\|\beta\|_1 = \sum_{(j,k) \in \vec{E}} |\beta_{jk}|$) with a particular choice of the ℓ_1 penalty. This motivates us to consider tighter continuous relaxation for MIQP. Let (β^R, g^R) be an optimal solution to the continuous relaxation of MIQP.

Proposition 5. *For $M \geq 2 \max_{(j,k) \in \vec{E}} |\beta_{jk}^R|$, a continuous relaxation of MIQP (16), where the binary variables are relaxed, is equivalent to the problem where the ℓ_0 regularization term is replaced with an ℓ_1 -regularization term with penalty parameter $\tilde{\lambda} = \frac{\lambda_n}{M}$.*

Proof. For $M \geq 2 \max_{(j,k) \in \vec{E}} |\beta_{jk}^R|$, the value g_{jk}^R is $\frac{\beta_{jk}^R}{M}$ in an optimal solution to the continuous relaxation of MIQP (16). Otherwise, we can reduce the value of the decision variable g^R without violating any constraints while reducing the objective function. Note that since $M \geq 2 \max_{(j,k) \in \vec{E}} |\beta_{jk}^R|$,

we have $\frac{\beta_{jk}^R}{M} \leq 1, \forall (j, k) \in \vec{E}$. To show that the set of constraints in (10b) is satisfied, we consider the set of CP constraints. In this case, the set of constraints (10b) holds, i.e., $\sum_{(j,k) \in \mathcal{C}_A} \frac{\beta_{jk}^R}{M} \leq |\mathcal{C}_A| - 1, \forall \mathcal{C}_A \in \mathcal{C}$, because $M \geq 2 \max_{(j,k) \in \vec{E}} |\beta_{jk}^R|$. This implies that $g_{jk}^R = \frac{\beta_{jk}^R}{M}$ is the optimal solution.

Thus, the objective function reduces to ℓ_1 regularization with the coefficient $\frac{\lambda_n}{M}$.

Finally, Proposition 4 establishes that for $M \geq 2 \max_{(j,k) \in \vec{E}} |\beta_{jk}^*|$, the objective function value of

the continuous relaxations of MIQP+CP, MIQP+LN and MIQP+TO are equivalent. This implies that the continuous relaxations of all formulations are equivalent, which completes the proof. \square

Despite the promising performance of MIQP+LN, its continuous relaxation objective function value provides a weak lower bound due to the big- M constraints. To circumvent this issue, a natural strategy is to improve the big- M value. Nonetheless, existing methods which ensure a valid big- M value or heuristic techniques [36, 24] do not lead to tight big- M values. For instance, the heuristic technique by [36] to obtain big- M values always satisfies the condition in Proposition 3 and exact techniques are expected to produce even larger big- M values. Therefore, we next directly develop tighter approximations for (10c).

5 New Perspectives for Mathematical Formulations of DAG Learning

In this section, we discuss improved mathematical formulations for learning DAG structure of a BN based on convex (instead of linear) encodings of the constraints in (10c).

Problem (10) is an MIQP with non-convex complementarity constraints (10c), a class of problems which has received a fair amount of attention from the operations research community over the last decade [17, 18, 19, 20, 24]. There has also been recent interest in leveraging these developments to solve sparse regression problems with ℓ_0 regularization [39, 15, 53, 3, 51].

Next, we review applications of MIQPs with complementarity constraints of the form (10c) for solving sparse regression with ℓ_0 regularization. [20] develop a so-called projected perspective relaxation method, to solve the perspective relaxation of mixed-integer nonlinear programming problems with a convex objective function and complementarity constraints. This reformulation requires that the corresponding binary variables are not involved in other constraints. Therefore, it is suitable for ℓ_0 sparse regression, but cannot be applied for DAG structure learning. [39] show how a broad class of ℓ_0 -regularized problems, including sparse regression as a special case, can be formulated exactly as optimization problems. The authors use the Tikhonov regularization term $\mu\|\beta\|_2^2$ and convex analysis to construct an improved convex relaxation using the reverse Huber penalty. In a similar vein, [6] exploit the Tikhonov regularization and develop an efficient algorithm by reformulating the sparse regression mathematical formulation as a saddle-point optimization problem with an outer linear integer optimization problem and an inner dual quadratic optimization problem which is capable of solving high-dimensional sparse regressions. [53] apply the perspective formulation of sparse regression optimization problem with both ℓ_0 and the Tikhonov regularization. The authors establish that the continuous relaxation of the perspective formulation is equivalent to the continuous relaxation of the formulation given by [6]. [15] propose perspective relaxation for ℓ_0 sparse regression optimization formulation and establish that the popular sparsity-inducing concave penalty function known as the minimax concave penalty [54] and the reverse Huber penalty [39] can be obtained as special cases of the perspective relaxation – thus the relaxations of formulations by [54, 39, 6, 53] are equivalent. The authors obtain an optimal perspective relaxation that is no weaker than any perspective relaxation. Among the related approaches, the optimal perspective relaxation by [15] is the only one that does not explicitly require the use of Tikhonov regularization.

The perspective formulation, which in essence is a fractional non-linear program, can be cast either as a mixed-integer second-order cone program (MISOCP) or a semi-infinite mixed-integer linear program (SIMILP). Both formulations can be solved directly by state-of-the-art optimization

packages. [15] and [3] solve the continuous relaxations and then use a heuristic approach (e.g., rounding techniques) to obtain a feasible solution (an upper bound). In this paper, we directly solve the MISOCP and SIMILP formulations for learning sparse DAG structures.

Next, we present how perspective formulation can be suitably applied for DAG structure learning with ℓ_0 regularization. We further cast the problem as MISOCP and SIMILP. To this end, we express the objective function (15a) in the following way:

$$\text{tr}[(I - B)(I - B)^\top \mathcal{X}^\top \mathcal{X}] + \lambda_n \sum_{(j,k) \in \vec{E}} g_{jk} \quad (16a)$$

$$= \text{tr}[(I - B - B^\top) \mathcal{X}^\top \mathcal{X} + 2BB^\top \mathcal{X}^\top \mathcal{X}] + \lambda_n \sum_{(j,k) \in \vec{E}} g_{jk}. \quad (16b)$$

Let $\delta \in \mathbb{R}_+^m$ be a vector such that $\mathcal{X}^\top \mathcal{X} - D_\delta \succeq 0$, where $D_\delta = \text{diag}(\delta_1, \dots, \delta_m)$ and $A \succeq 0$ means that matrix A is positive semi-definite. By splitting the quadratic term $\mathcal{X}^\top \mathcal{X} = (\mathcal{X}^\top \mathcal{X} - D_\delta) + D_\delta$ in (16b), the objective function can be expressed as

$$\text{tr}[(I - B - B^\top) \mathcal{X}^\top \mathcal{X} + BB^\top (\mathcal{X}^\top \mathcal{X} - D_\delta)] + \text{tr}(BB^\top D_\delta) + \lambda_n \sum_{(j,k) \in \vec{E}} g_{jk}. \quad (17)$$

Let $Q = \mathcal{X}^\top \mathcal{X} - D_\delta$. (In the presence of Tikhonov regularization with tuning parameter $\mu > 0$, we let $Q = \mathcal{X}^\top \mathcal{X} + \mu I - D_\delta$ as described in Remark 1.) Then, Cholesky decomposition can be applied to decompose Q as $q^\top q$ (note $Q \succeq 0$). As a result, $\text{tr}(BB^\top Q) = \text{tr}(BB^\top q^\top q) = \sum_{i=1}^m \sum_{j=1}^m \left(\sum_{(\ell,j) \in \vec{E}} \beta_{\ell j} q_{i\ell} \right)^2$. The separable component can also be expressed as $\text{tr}(BB^\top D_\delta) = \sum_{j=1}^m \sum_{(j,k) \in \vec{E}} \delta_j \beta_{jk}^2$. Using this notation, the objective (17) can be written as

$$\text{tr}[(I - B - B^\top) \mathcal{X}^\top \mathcal{X} + BB^\top Q] + \sum_{j=1}^m \sum_{(j,k) \in \vec{E}} \delta_j \beta_{jk}^2 + \lambda_n \sum_{(j,k) \in \vec{E}} g_{jk}.$$

The Perspective Reformulation (PRef) of MIQP is then given by

$$\mathbf{PRef} \quad \min \quad \text{tr}[(I - B - B^\top) \mathcal{X}^\top \mathcal{X} + BB^\top Q] + \quad (18a)$$

$$\sum_{j=1}^m \sum_{(j,k) \in \vec{E}} \delta_j \frac{\beta_{jk}^2}{g_{jk}} + \lambda_n \sum_{(j,k) \in \vec{E}} g_{jk}, \quad (18b)$$

(15b) – (15c).

The objective function (18a) is formally undefined when some $g_{jk} = 0$. More precisely, we use the convention that $\frac{\beta_{jk}^2}{g_{jk}} = 0$ when $\beta_{jk} = g_{jk} = 0$ and $\frac{\beta_{jk}^2}{g_{jk}} = +\infty$ when $\beta_{jk} \neq 0$ and $g_{jk} = 0$ [19]. The continuous relaxation of PRef, referred to as the perspective relaxation, is much stronger than the continuous relaxation of MIQP [39]. However, an issue with PRef is that the objective function is nonlinear due to the fractional term. There are two ways to reformulate PRef. One as a mixed-integer second-order conic program (MISOCP) (see, Section 5.1) and the other as a semi-infinite mixed-integer linear program (SIMILP) (see, Section 5.2).

5.1 Mixed-integer second-order conic program

Let s_{jk} be additional variables representing β_{jk}^2 . Then, the MISOCP formulation is given by

$$\text{MISOCP} \quad \min \quad \text{tr}[(I - B - B^\top)\mathcal{X}^\top \mathcal{X} + BB^\top Q] + \quad (19a)$$

$$\sum_{j=1}^m \sum_{(j,k) \in \vec{E}} \delta_j s_{jk} + \lambda_n \sum_{(j,k) \in \vec{E}} g_{jk},$$

$$s_{jk} g_{jk} \geq \beta_{jk}^2 \quad (j, k) \in \vec{E}, \quad (19b)$$

$$0 \leq s_{jk} \leq M^2 g_{jk} \quad (j, k) \in \vec{E}, \quad (19c)$$

$$(15b) - (15c). \quad (19d)$$

Here, the constraints in (19b) imply that $\beta_{jk} \neq 0$ only when $z_{jk} = 1$. The constraints in (19b) are second-order conic representable because they can be written in the form of $\sqrt{4\beta_{jk}^2 + (s_{jk} - g_{jk})^2} \leq s_{jk} + g_{jk}$. The set of constraints in (19c) is valid since $\beta_{jk} \leq M g_{jk}$ implies $\beta_{jk}^2 \leq M^2 g_{jk}^2 = M^2 g_{jk}^2$ and $g_{jk}^2 = g_{jk}$ for $g_{jk} \in \{0, 1\}$. The set of constraints in (19c) is not required, yet they improve the computational efficiency especially when we restrict the big- M value. [53] report similar behavior for sparse regression. When we relax $g_{jk} \in \{0, 1\}$ and let $g_{jk} \in [0, 1]$, we obtain the continuous relaxation of MISOCP (19). Let us denote the feasible region of continuous relaxation of MISOCP (19) and MIQP (16) by $\mathcal{RMISOCP}$ and \mathcal{RMIQP} , and the objective function values by $\text{OFV}(\mathcal{RMISOCP})$ and $\text{OFV}(\mathcal{RMIQP})$, respectively. For a more general problem than ours, [10] give a detailed proof establishing that the feasible region of the former is contained in the feasible region of latter i.e., $\mathcal{RMISOCP} \subset \mathcal{RMIQP}$. This implies that $\text{OFV}(\mathcal{RMISOCP}) \not\geq \text{OFV}(\mathcal{RMIQP})$. Therefore, we are able to obtain stronger lower bounds using MISOCP than MIQP.

5.2 Mixed-integer semi-infinite integer linear program

An alternative approach to reformulate PRef is via *perspective cuts* developed by [17, 18]. To apply perspective cuts, we use the reformulation idea first proposed in [17] by introducing dummy decision matrix D to distinguish the separable and non-separable part of the objective function; we also add the additional constraint $d = \beta$ where d_{jk} is (j, k) element of matrix D and β is the decision variable in the optimization problem. Following this approach, MIQP can be reformulated as an SIMILP:

$$\text{SIMILP} \quad \min \quad \text{tr}[(I - B - B^\top)\mathcal{X}^\top \mathcal{X} + DD^\top Q] + \quad (20a)$$

$$\sum_{j=1}^m \sum_{(j,k) \in \vec{E}} \delta_j v_{jk} + \lambda_n \sum_{(j,k) \in \vec{E}} g_{jk},$$

$$d_{jk} = \beta_{jk} \quad (j, k) \in \vec{E}, \quad (20b)$$

$$v_{jk} \geq 2\bar{\beta}_{jk}\beta_{jk} - \bar{\beta}_{jk}^2 g_{jk} \quad \forall \bar{\beta}_{jk} \in [-M, M] \quad \forall (j, k) \in \vec{E}, \quad (20c)$$

$$(15b) - (15c), \quad (20d)$$

$$v_{jk} \geq 0, \quad (j, k) \in \vec{E}. \quad (20e)$$

The set of constraints in (20c) are known as perspective cuts. Note that there are infinitely many such constraints. Although this problem cannot be solved directly, it lends itself to a delayed cut

generation approach whereby a (small) finite subset of constraints in (20c) is kept, the current solution (β^*, g^*, v^*) of the relaxation is obtained, and all the violated inequalities for the relaxation solution are added for $\bar{\beta}_{jk} = \frac{\beta_{jk}^*}{g_{jk}^*}$ (assuming $\frac{0}{0} = 0$). This process is repeated until termination criteria are met. This procedure can be implemented using the cut callback function available by off-the-shelf solvers such as Gurobi or CPLEX.

5.3 Selecting δ

In the MISOCP and SIMILP formulations, one important question is how to identify a valid δ . A natural choice is $\text{diag}(\delta) = (\lambda_{\min} - \varepsilon)e$ where λ_{\min} is the minimum eigenvalue of $\mathcal{X}^\top \mathcal{X}$, $\varepsilon > 0$ is a sufficiently small number to avoid numerical instability of estimating eigenvalues, and e is a column vector of ones. The issue with this approach is that if $\lambda_{\min} = 0$, then $\text{diag}(\delta)$ becomes a trivial 0 matrix. If $\text{diag}(\delta)$ turns out to be a zero matrix, then MISOCP formulation reduces to the big- M formulation. [18] present an effective approach for obtaining a valid δ by solving the following semidefinite program (SDP)

$$\max \left\{ \sum_{i \in V} \delta_i \mid \mathcal{X}^\top \mathcal{X} - \text{diag}(\delta) \succeq 0, \delta_i \geq 0 \right\}. \quad (21a)$$

This formulation can attain a non-zero D_δ even if $\lambda_{\min} = 0$. Numerical results by [18] show that this method compares favorably with the minimum eigenvalue approach. [55] propose an SDP approach, which obtains D_δ such that the continuous relaxation of MISOCP (19) is as tight as possible.

Similar to [15], our formulation does not require adding a Tikhonov regularization. In this case, PRef is effective when $\mathcal{X}^\top \mathcal{X}$ is sufficiently diagonally dominant. When $n \geq m$ and each row of \mathcal{X} is independent, then $\mathcal{X}^\top \mathcal{X}$ is guaranteed to be a positive semi-definite matrix [15]. On the other hand, when $n < m$, $\mathcal{X}^\top \mathcal{X}$ is not full-rank. Therefore, a Tikhonov regularization term should be added with sufficiently large μ to make $\mathcal{X}^\top \mathcal{X} + \mu I \succeq 0$ [15] in order to benefit from the strengthening provided by PRef.

6 Experiments

In this section, we report the results of our numerical experiments that compare different formulations and evaluate the effect of different tuning parameters and estimation strategies. Our experiments are performed on a cluster operating on UNIX with Intel Xeon E5-2640v4 2.4GHz. All formulations are implemented in the Python programming language. Gurobi 8.1 is used as the solver. Unless otherwise stated, a time limit of 50m (in seconds), where m denotes the number of nodes, and an MIQP relative optimality gap of 0.01 are imposed across all experiments after which runs are aborted. The *relative* optimality gap is calculated by $\text{RGAP} := \frac{\text{UB}(X) - \text{LB}(X)}{\text{UB}(X)}$ where $\text{UB}(X)$ denotes the objective value associated with the best feasible integer solution (incumbent) and $\text{LB}(X)$ represents the best obtained lower bound during the branch-and-bound process for the formulation $X \in \{\text{MIQP}, \text{SIMILP}, \text{MISOCP}\}$.

Unless otherwise stated, we assume $\lambda_n = \ln(n)$ which corresponds to the Bayesian information criterion (BIC) score. To select the big- M parameter, M , in all formulations we use the proposal of Park and Klabjan [36]. Specifically, given λ_n , we solve each problem without cycle prevention

constraints and obtain β^R . We then use the upper bound $M = 2 \max_{(j,k) \in \vec{E}} |\beta_{jk}^R|$. Although this value does not guarantee an upper bound for M , the results provided in [36] and [30] computationally confirm that this approach gives a large enough value of M .

The goals of our computational study are twofold. First, we compare the various mathematical formulations to determine which gives us the best performance in Subsection 6.1, compare the sensitivity to the model parameters in Subsection 6.2, and the choice of the regularization term in Subsection 6.3. Second, in Subsection 6.4 we use the best-performing formulation to investigate the implications of the early stopping condition on the quality of the solution with respect to the true graph. To be able to perform such a study, we use synthetic data so that the true graph is available.

We use the package `pcalg` in R to generate random graphs. First, we create a DAG by `randomDAG` function and assign random arc weights (i.e., β) from a uniform distribution, $\mathcal{U}[0.1, 1]$. Next, the resulting DAG and random coefficients are fed into the `rmvDAG` function to generate multivariate data based on linear SEMs (columns of matrix \mathcal{X}) with the standard normal error distribution. We consider $m \in \{10, 20, 30, 40\}$ nodes and $n = 100$ samples. The average outgoing degree of each node, denoted by d , is set to two. We generate 10 random Erdős-Rényi graphs for each setting (m , n , d). We observe that in our instances, the minimum eigenvalue of $\mathcal{X}^\top \mathcal{X}$ across all instances is 3.26 and the maximum eigenvalue is 14.21.

Two types of problem instances are considered: (i) a set of instances with known moral graph corresponding to the true DAG; (ii) a set of instances with a complete undirected graph, i.e., assuming no prior knowledge. We refer to the first class of instances as *moral* instances and to the second class as *complete* instances. The observational data, \mathcal{X} , for both classes of instances are the same. The function `moralize(graph)` in the `pcalg` R-package is used to generate the moral graph from the true DAG. Although the moral graph can be consistently estimated from data using penalized estimation procedures with polynomial complexity [e.g., 29], the quality of moral graph affects all optimization models. Therefore, we use the true moral graph in our experiments.

6.1 Comparison of Mathematical Formulations

We use the following MIQP-based metrics to measure the quality of a solution: relative optimality gap (RGAP), computation time in seconds (Time), Upper Bound (UB), Lower Bound (LB), objective function value (OFV) of the initial continuous relaxation, and the number of explored nodes in the branch-and-bound tree (# BB). An in-depth analysis comparing the existing mathematical formulations that rely on linear encodings of the constraints in (10c) for MIQP formulations is conducted by [30]. The authors conclude that MIQP+LN formulation outperforms the other MIQP formulations, and the promising performance of MIQP+LN can be attributed to its size: (1) MIQP+LN has fewer binary variables and constraints than MIQP+TO, (2) MIQP+LN is a compact (polynomial-sized) formulation in contrast to MIQP+CP which has an exponential number of constraints. Therefore, in this paper, we analyze the formulations based on the convex encodings of the constraints in (10c).

6.1.1 Comparison of MISOCP formulations

We next experiment with MISOCP formulations. For the set of constraints in (10b), we use LN, TO, and CP constraints discussed in Section 4.1 resulting in three formulations denoted as MISOCP+LN, MISOCP+TO, MISOCP+CP, respectively. The MISOCP+TO formulation fails to find

Table 1: Optimality gaps for MISOCP+TO and MISOCP+LN formulations

m	Moral		Complete	
	MISOCP+TO	MISOCP+LN	MISOCP+TO	MISOCP+LN
10	0.000	0.000	0.009	0.008
20	0.021	0.006	0.272	0.195
30	-	0.010	-	0.195
40	-	0.042	-	0.436

“-” denotes that no feasible solution, i.e., UB, is obtained within the time limit, so optimality gap cannot be computed.

a feasible solution for instances with 30 and 40 nodes, see Table 1. For moral instances, the optimality gap for MISOCP+TO are 0.000 and 0.021 for instances with 10 and 20 nodes, respectively; for complete instances, the optimality gap for MISOCP+TO formulation are 0.009 and 0.272 for instances with 10 and 20 nodes, respectively. Moreover, Table 1 illustrates that MISOCP+LN performs better than MISOCP+TO for even small instances (i.e., 10 and 20 nodes).

For MISOCP+CP, instead of incorporating all constraints given by (11), we begin with no constraint of type (11). Given an integer solution with cycles, we detect a cycle and impose a new cycle prevention constraint to remove the detected cycle. Depth First Search (DFS) can detect a cycle in a directed graph with complexity $O(|V| + |E|)$. Gurobi `LazyCallback` function is used, which allows adding cycle prevention constraints in the branch-and-bound algorithm, whenever an integer solution with cycles is found. The same approach is used by [36] to solve the corresponding MIQP+CP. Note that Gurobi solver follows a branch-and-cut implementation and adds many general-purpose and special-purpose cutting planes.

Figures 1a and 1b show that MISOCP+LN outperforms MISOCP+CP in terms of relative optimality gap and computational time. In addition, MISOCP+LN attains better upper and lower bounds than MISOCP+CP (see, Figures 1c and 1d). MISOCP+CP requires the solution of a second-order cone program (SOCP) after each cut, which reduces its computational efficiency and results in higher optimality gaps than MISOCP+LN. MISOCP+TO requires many binary variables which makes the problem very inefficient when the network becomes denser and larger as shown in Table 1. Therefore, we do not illustrate the MISOCP+TO results in Figure 1.

6.1.2 Comparison of MISOCP versus SIMILP

Our computational experiments show that the SIMILP formulation generally performs poorly when compared to MISOCP+LN and MIQP+LN in terms of optimality gap, upper bound, and computational time. We report the results for SIMILP+LN, MISOCP+LN, and MIQP+LN formulations in Figure 2. We only consider the LN formulation because that is the best performing model among the alternatives both for MISOCP and MIQP formulations.

Figures 2a and 2b show the relative optimality gaps and computational times for these three formulations. Figures 2c and 2d demonstrate that SIMILP+LN attains lower bounds that are comparable with other two formulations. In particular, for complete instances with large number of nodes, SIMILP+LN attains better lower bounds than MIQP+LN. Nonetheless, SIMILP+LN fails to obtain good upper bounds. Therefore, the relative optimality gap is considerably larger for SIMILP+LN.

The poor performance of SIMILP+LN might be because state-of-the-art optimization packages (e.g., Gurobi, CPLEX) use many heuristics to obtain a good feasible solution (i.e., upper bound) for a compact formulation. In contrast, SIMILP is not a compact formulation, and we build the

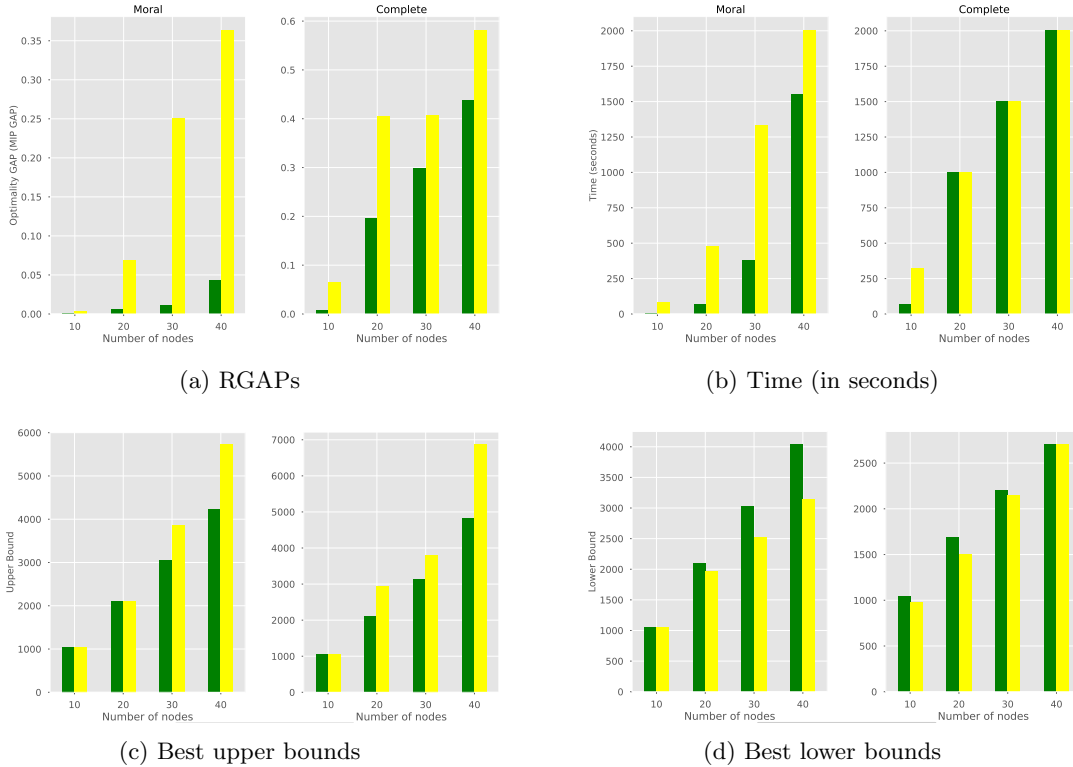


Figure 1: Optimization-based measures for MISOCP+LN (green, left bar) and MISOCP+CP (yellow, right bar) formulations for $n = 100$ and $\lambda_n = \ln(n)$.

SIMILP gradually by adding violated constraints iteratively. Therefore, a feasible solution to the original formulation is not available while solving the relaxations with a subset of the constraints (20c). Moreover, the optimization solvers capable of solving MISOCP formulations have witnessed noticeable improvement due to theoretical developments in this field. In particular, Gurobi reports 20% and 38% improvement in solution time for versions 8 and 8.1, respectively. In addition, Gurobi v8.1 reports over four times faster solution times than CPLEX for solving MISOCP on their benchmark instances.

6.1.3 Comparison of MISOCP versus MIQP formulations

In this section, we demonstrate the benefit of using the second-order conic formulation MISOCP+LN instead of the linear big- M formulation MIQP+LN. As before, we only consider the LN formulation for this purpose. Figures 3a and 3b show that MISOCP+LN performs better than MIQP+LN in terms of the average relative optimality gap across all number of nodes $m \in \{10, 20, 30, 40\}$. The only exception is $m = 40$ for moral instances, for which MIQP+LN performs better than MISOCP+LN. Nonetheless, we observe that MISOCP+LN clearly outperforms MIQP+LN for complete instances which are more difficult to solve.

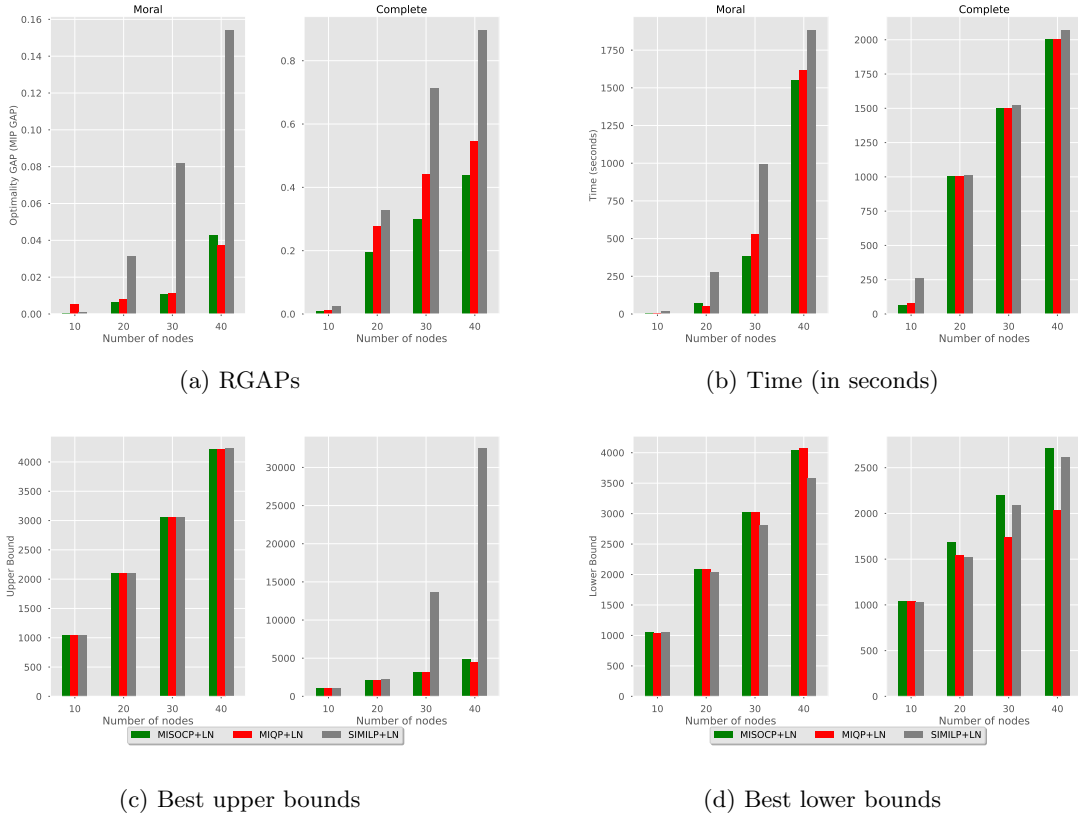


Figure 2: Optimization-based measures for **MISOCP+LN**, **MIQP+LN**, and **MISILP+LN** formulations for $n = 100$ and $\lambda_n = \ln(n)$.

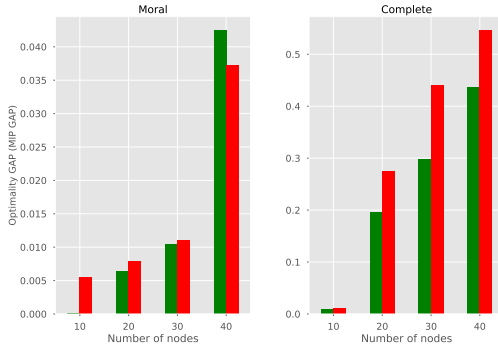
Figures 3c and 3d show the performance of both formulations in terms of the resulting upper and lower bounds on the objective function. We observe that **MISOCP+LN** attains better lower bounds especially for complete instances. However, **MISOCP+LN** cannot always obtain a better upper bound. In other words, **MISOCP+LN** is more effective in improving the lower bound instead of the upper bound as expected.

Figures 3e and 3f show that **MISOCP+LN** uses fewer branch-and-bound nodes and achieves better continuous relaxation values than **MIQP+LN**.

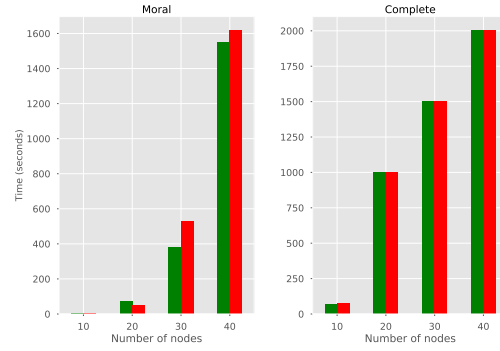
6.2 Analyzing the Choices of λ_n and M

We now experiment on different values for λ_n and M to assess the effects of these parameters on the performance of **MISOCP+LN** and **MIQP+LN**. First, we change $\lambda_n \in \{\ln(n), 2\ln(n), 4\ln(n)\}$ while keeping the value of M the same (i.e., $M = 2 \max_{(j,k) \in \vec{E}} |\beta_{jk}^*|$). Table 2 shows that as λ_n increases, **MIS-**

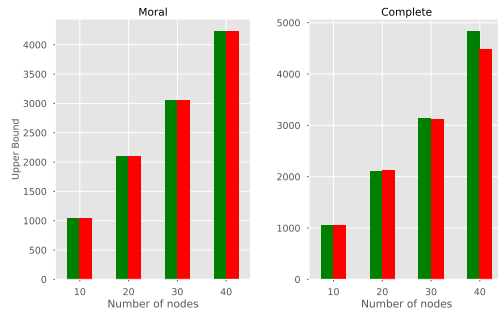
OCP+LN consistently performs better than **MIQP+LN** in terms of the relative optimality gap, computational time, the number of branch-



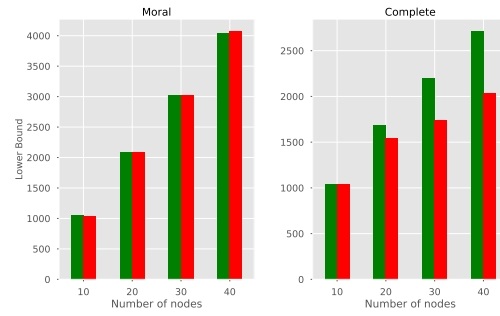
(a) RGAPs



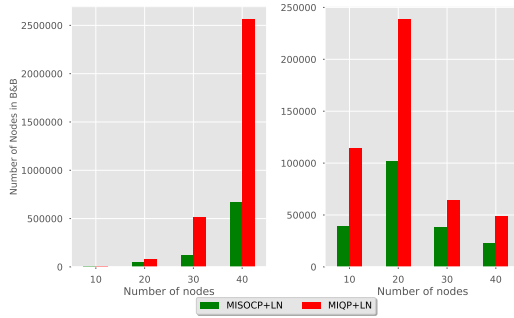
(b) Time (in seconds)



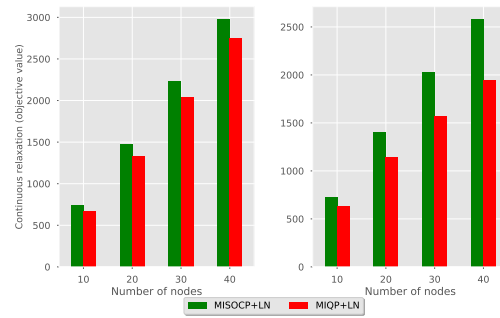
(c) Best upper bounds



(d) Best lower bounds



(e) Number of Branch and Bound nodes



(f) Continuous relaxation objective function

Figure 3: Optimization-based measures for **MISOCPLN**, **MIQPLN** formulations for $n = 100$ and $\lambda_n = \ln(n)$.

and-bound nodes, and continuous relaxation objective function value. Indeed, the difference becomes even more pronounced for more difficult cases (i.e., complete instances). For instance, for

Table 2: Computational results for different values of $\lambda_n = t \ln(n)$ for $t \in \{1, 2, 4\}$

		Moral								Complete							
Instances m	λ_n	RGAP		Time		# nodes		Relaxation OFV		RGAP		Time		# nodes		Relaxation OFV	
		MISOCP	MIQP	MISOCP	MIQP	MISOCP	MIQP	MISOCP	MIQP	MISOCP	MIQP	MISOCP	MIQP	MISOCP	MIQP	MISOCP	MIQP
10	4.6	*	*	3	2	1306	3715	738.7	664.9	*	*	65	74	38850	114433	724.4	629.3
10	9.2	*	*	4	3	1116	2936	784.6	693.5	*	*	31	39	15736	55543	772.5	662.2
10	18.4	*	*	3	2	1269	2457	857.0	747.5	*	*	26	29	18223	41197	844.5	720.2
20	4.6	*	*	69	51	46513	76261	1474.2	1325.8	0.195	0.275	1000	1000	101509	238765	1404.9	1144.5
20	9.2	*	*	26	27	10695	31458	1589.6	1406.8	0.152	0.250	1000	1000	152206	274514	1526.9	1238.6
20	18.4	*	*	24	36	9574	33788	1763.7	1552.7	0.113	0.208	944	1000	159789	277687	1697.1	1395.0
30	4.6	0.010	0.011	378	527	121358	514979	2230.1	2037.7	0.298	0.441	1500	1500	38474	64240	2024.0	1569.7
30	9.2	*	*	104	291	33371	248190	2392.4	2168.5	0.239	0.395	1500	1500	59034	71475	2217.5	1741.5
30	18.4	*	*	48	74	15649	57909	2608.3	2383.8	0.215	0.318	1500	1500	74952	96586	2449.2	2006.9
40	4.6	0.042	0.037	1551	1615	664496	2565247	2979.3	2748.6	0.436	0.545	2000	2000	23083	49050	2582.0	1946.3
40	9.2	0.024	0.036	1125	1336	353256	1347702	3200.7	2923.5	0.397	0.473	2000	2000	29279	73917	2869.9	2216.9
40	18.4	0.024	0.035	1099	1375	434648	1137666	3521.8	3225.4	0.374	0.465	2000	2000	31298	60697	3240.1	2633.1

* indicates that the problem is solved to the optimality tolerance.
Better RGAPs are in bold.

Table 3: Computational results for different values of γ

		Moral								Complete							
Instances m	γ	RGAP		Time		# nodes		Relaxation OFV		RGAP		Time		# nodes		Relaxation OFV	
		MISOCP	MIQP	MISOCP	MIQP	MISOCP	MIQP	MISOCP	MIQP	MISOCP	MIQP	MISOCP	MIQP	MISOCP	MIQP	MISOCP	MIQP
10	2	*	*	3	2	1306	3715	738.7	664.9	*	*	65	74	38850	114433	724.4	629.3
10	5	*	*	5	2	1433	3026	717.9	647.1	*	*	81	82	42675	130112	705.1	607.8
10	10	*	*	5	2	1523	2564	712.5	641.1	*	*	74	100	35576	174085	699.8	600.3
20	2	*	*	69	51	46513	76261	1474.2	1325.8	0.195	0.275	1000	1000	101509	238765	1404.9	1144.5
20	5	*	*	103	156	65951	209595	1438.2	1274.2	0.211	0.308	1000	1000	97940	225050	1375.3	1080.9
20	10	*	*	215	207	150250	349335	1427.7	1256.6	0.230	0.310	1000	1000	90864	257998	1366.3	1058.2
30	2	0.010	0.011	378	527	121358	514979	2230.1	2037.7	0.298	0.441	1500	1500	38474	64240	2024.0	1569.7
30	5	0.011	0.014	571	620	164852	527847	2173.9	1950.3	0.336	0.474	1501	1500	33120	64339	1969.4	1448.4
30	10	0.024	0.014	630	638	202635	585234	2156.5	1919.6	0.349	0.480	1500	1500	30579	77100	1951.2	1404.0
40	2	0.042	0.037	1551	1615	664496	2565247	2979.3	2748.6	0.436	0.545	2000	2000	23083	49050	2582.0	1946.3
40	5	0.045	0.047	1643	1634	638323	1347868	2895.6	2635.0	0.579	0.580	2000	2000	12076	30858	2488.0	1751.7
40	10	0.056	0.057	1639	1632	599281	1584187	2869.2	2595.6	0.585	0.594	2000	2000	11847	30222	2456.1	1679.6

* indicates that the problem is solved to the optimality tolerance.
Better RGAPs are in bold.

$\lambda_n = 4 \ln(n) = 18.4$, the optimality gap reduces from 0.465 to 0.374, an over 24% improvement.

Finally, we study the influence of the big- M parameter. Instead of a coefficient $\gamma = 2$ in [36], we experiment with $M = \gamma \max_{(j,k) \in \vec{E}} |\beta_{jk}^R|$ for $\gamma \in \{2, 5, 10\}$ in Table 3, where $|\beta_{jk}^R|$ denotes the optimal

solution of each optimization problem without the constraints to remove cycles. The larger the big- M parameter, the worse the effectiveness of both models. However, MISOCP+LN tightens the formulation using the conic constraints whereas MIQP+LN does not have any means to tighten the formulation instead of big- M constraints which have poor relaxation. For $M > 2 \max_{(j,k) \in \vec{E}} |\beta_{jk}^R|$,

MISOCP+LN outperforms MIQP+LN in all measures, in most cases.

Table 4: Computational results for different values of μ

		Moral								Complete							
Instances m μ	RGAP		Time		# nodes		Relaxation OFV		MISOCP	MIQP	MISOCP	MIQP	# nodes	Relaxation OFV	MISOCP	MIQP	
	MISOCP	MIQP	MISOCP	MIQP	MISOCP	MIQP	MISOCP	MIQP									MISOCP
10 0	*	*	3	2	1306	3715	738.7	664.9	*	*	65	74	38850	114433	724.4	629.3	
10 4.6	*	*	4	2	1043	2758	802.0	708.5	*	*	69	72	38778	119825	789.3	675.7	
10 9.2	*	*	4	2	1067	2231	858.0	748.1	*	*	72	74	36326	114383	843.2	712.3	
20 0	*	*	69	51	46513	76261	1474.2	1325.8	0.195	0.2752	1000	1000	101509	238765	1404.9	1144.5	
20 4.6	*	*	45	45	15111	55302	1604.1	1426.5	0.1666	0.2416	1000	1000	102467	249490	1551.7	1267.1	
20 9.2	*	*	43	55	15384	62297	1716.8	1515.7	0.1422	0.2228	1000	1000	94360	258194	1668.3	1355.1	
30 0	0.010	0.011	378	527	121358	514979	2230.1	2037.7	0.298	0.4408	1500	1500	38474	64240	2024.0	1569.7	
30 4.6	0.008	0.011	310	392	76668	358544	2432.5	2187.7	0.2368	0.387	1500	1500	45473	69258	2286.4	1788.5	
30 9.2	0.009	0.010	67	377	12410	320632	2612.6	2311.4	0.2092	0.3666	1500	1500	41241	68661	2484.3	1915.7	
40 0	0.042	0.037	1551	1615	664496	2565247	2979.3	2748.6	0.4364	0.5452	2000	2000	23083	49050	2582.0	1946.3	
40 4.6	0.027	0.029	1331	1620	422654	1303301	3281.6	2972.8	0.3538	0.4708	2000	2000	13209	30995	2985.4	2261.3	
40 9.2	0.020	0.028	870	1507	239214	1762210	3575.4	3165.3	0.3668	0.4454	2000	2000	13884	54638	3321.7	2468.7	

* indicates that the problem is solved to the optimality tolerance.
 Better RGAPs are in bold.

6.3 The Effect of Tikhonov Regularization

In this subsection, we consider the effect of adding a Tikhonov regularization term to the objective (see Remark 1) by considering $\mu \in \{0, \ln(n), 2\ln(n)\}$ while keeping the values of $\lambda_n = \ln(n)$ and M the same as before. Table 4 demonstrates that for all instances with $\mu > 0$, MISOCP+LN outperforms MIQP+LN. For instance, for $m = 40$ and $\mu = 18.4$, MISOCP+LN improves the optimality gap from 0.445 to 0.366, an improvement over 21%. The reason for this improvement is that $\mu > 0$ makes the matrix more diagonally dominant; therefore, it makes the conic constraints more effective in tightening the formulation and obtaining a better optimality gap.

6.4 Practical Implications of Early Stopping

In this subsection, we evaluate the quality of the estimated DAGs obtained from MISOCP+LN by comparing them with the ground truth DAG. To this end, we use the average structural Hamming distance (SHD) which counts the number of arc differences (additions, deletions, or reversals) required to transform the estimated DAG to the true DAG. Since Gurobi sets a minimum relative gap $RGAP = 1e^{-4}$, the solution obtained within this relative gap is considered optimal. Finally, because the convergence of the branch-and-bound process may be slow in some cases, we set a time limit of $100m$.

To test the quality of the solution obtained with an early stopping criterion, we set the absolute optimality gap parameter as $GAP = \frac{\log(m)}{n} s_m$ and the ℓ_0 regularization parameter as $\lambda_n = \log m$ as suggested by Proposition 2 for achieving a consistent estimate. We compare the resulting suboptimal solution to the solution obtained by setting $GAP = UB - LB = 0$ to obtain the truly optimal solution.

Table 5 shows the numerical results for the average solution time (in seconds) for instances that solve within the time limit, the number of instances that were not solved within the time limit, the actual absolute optimality gap at termination, the average SHD of the resulting DAGs, and in parenthesis, the standard deviation of the SHD scores, across 10 runs for moral instances. Table 5 indicates that the average SHD for $GAP = \frac{\log(m)}{n} s_m$ is close to that of the truly optimal solution. Note that a lower GAP does not necessarily lead to a better SHD score; see, e.g., $m = 20$. From

Table 5: Structural Hamming distances (SHD) for early stopping with $n = 100$, $\lambda_n = \log m$, $\text{GAP} \leq \tau$ for moral instances. The superscripts i indicate that out of ten runs, i instances reach the time limit of $100m$.

		$\tau = 0$			$\tau = \frac{\log(m)}{n} s_m$		
m	s_m	Time	GAP	SHD (std)	Time	GAP	SHD (std)
10	19	0.71	0.002	0 (0)	0.64	0.002	0 (0)
20	58	31.99	0.062	0.80 (1.23)	16.84	0.165	0.55 (1.01)
30	109	51.41 ²	0.210	1.25 (0.89)	28.27 ²	0.557	1.29 (0.95)
40	138	784.85 ⁴	0.370	0.67 (0.52)	1547.90 ²	1.411	0.71 (0.49)

a computational standpoint, we observe that by using the early stopping criterion, we are able to obtain consistent solutions before reaching the time limit for more instances. In particular, four instances reach the time limit for $\text{GAP}=0$ before finding the optimal solution as opposed to only two for early stopping, Note that we only report the average solution time if the algorithm terminates before hitting the time limit, which explains why the average time appears smaller for optimal than early stopping. Taking into account the time to obtain the best integer solution, the average time for $m = 40$ is 1678.485 seconds for $\text{GAP}=0$, whereas it is 954.79 seconds for the early stopping setting. Furthermore, stopping early does not sacrifice from the quality of the resulting DAG as can be seen from the SHD scores.

7 Conclusion

In this paper, we study the problem of learning an optimal directed acyclic graph (DAG) from continuous observational data, where the causal effect among the random variables is linear. The central problem is a quadratic optimization problem with regularization. We present a mixed-integer second order conic program (MISOCP) which entails a tighter relaxation than existing formulations with linear constraints. Our results show that MISOCP can successfully improve the lower bound and results in better optimality gap when compared with other formulations based on big- M constraints, especially for dense and large instances. Moreover, we establish an early stopping criterion under which we can terminate branch-and-bound and achieve a solution which is asymptotically optimal.

Acknowledgments

Simge Küçükyavuz and Linchuan Wei were supported, in part, by ONR grant N00014-19-1-2321. Ali Shojaie was supported by NSF grant DMS-1561814 and NIH grant R01GM114029.

References

- [1] Constantin F Aliferis, Alexander Statnikov, Ioannis Tsamardinos, Subramani Mani, and Xenofon D Koutsoukos. Local causal and Markov blanket induction for causal discovery and feature selection for classification part I: Algorithms and empirical evaluation. *Journal of Machine Learning Research*, 11(Jan):171–234, 2010.

- [2] Bryon Aragam and Qing Zhou. Concave penalized estimation of sparse Gaussian Bayesian networks. *Journal of Machine Learning Research*, 16:2273–2328, 2015.
- [3] Alper Atamtürk and Andres Gómez. Rank-one convexification for sparse regression. *arXiv preprint arXiv:1901.10334*, 2019.
- [4] Mark Barlett and James Cussens. Advances in bayesian network learning using integer programming. In *Proceedings of the Twenty-Ninth Conference on Uncertainty in Artificial Intelligence*, UAI’13, pages 182–191, Arlington, Virginia, USA, 2013. AUAI Press.
- [5] Mark Bartlett and James Cussens. Integer linear programming for the Bayesian network structure learning problem. *Artificial Intelligence*, 244:258–271, 2017.
- [6] Dimitris Bertsimas and Bart Van Parys. Sparse high-dimensional regression: Exact scalable algorithms and phase transitions. *The Annals of Statistics*, 48(1):300–323, 2020.
- [7] Dimitris Bertsimas, Angela King, and Rahul Mazumder. Best subset selection via a modern optimization lens. *The Annals of Statistics*, 44(2):813–852, 2016.
- [8] Peter Bühlmann and Sara A van de Geer. *Statistics for high-dimensional data: methods, theory and applications*. Springer, 2011.
- [9] Wenyu Chen, Mathias Drton, and Y Samuel Wang. On causal discovery with an equal-variance assumption. *Biometrika*, 106(4):973–980, 2019.
- [10] XT Cui, XJ Zheng, SS Zhu, and XL Sun. Convex relaxations and MIQCQP reformulations for a class of cardinality-constrained portfolio selection problems. *Journal of Global Optimization*, 56(4):1409–1423, 2013.
- [11] James Cussens. Maximum likelihood pedigree reconstruction using integer programming. In *WCB@ ICLP*, pages 8–19, 2010.
- [12] James Cussens. Bayesian network learning with cutting planes. In *Proceedings of the Twenty-Seventh Conference on Uncertainty in Artificial Intelligence*, UAI’11, pages 153–160, Arlington, Virginia, USA, 2011. AUAI Press.
- [13] James Cussens, David Haws, and Milan Studený. Polyhedral aspects of score equivalence in Bayesian network structure learning. *Mathematical Programming*, 164(1-2):285–324, 2017.
- [14] James Cussens, Matti Järvisalo, Janne H Korhonen, and Mark Bartlett. Bayesian network structure learning with integer programming: Polytopes, facets and complexity. *J. Artif. Intell. Res. (JAIR)*, 58:185–229, 2017.
- [15] Hongbo Dong, Kun Chen, and Jeff Linderoth. Regularization vs. relaxation: A conic optimization perspective of statistical variable selection. *arXiv preprint arXiv:1510.06083*, 2015.
- [16] Mathias Drton and Marloes H Maathuis. Structure learning in graphical modeling. *Annual Review of Statistics and Its Application*, 4:365–393, 2017.
- [17] Antonio Frangioni and Claudio Gentile. Perspective cuts for a class of convex 0–1 mixed integer programs. *Mathematical Programming*, 106(2):225–236, 2006.

- [18] Antonio Frangioni and Claudio Gentile. SDP diagonalizations and perspective cuts for a class of nonseparable MIQP. *Operations Research Letters*, 35(2):181–185, 2007.
- [19] Antonio Frangioni and Claudio Gentile. A computational comparison of reformulations of the perspective relaxation: SOCP vs. cutting planes. *Operations Research Letters*, 37(3):206–210, 2009.
- [20] Antonio Frangioni, Claudio Gentile, Enrico Grande, and Andrea Pacifici. Projected perspective reformulations with applications in design problems. *Operations Research*, 59(5):1225–1232, 2011.
- [21] Fei Fu and Qing Zhou. Learning sparse causal Gaussian networks with experimental intervention: regularization and coordinate descent. *Journal of the American Statistical Association*, 108(501):288–300, 2013.
- [22] Tian Gao, Ziheng Wang, and Qiang Ji. Structured feature selection. In *Proceedings of the IEEE International Conference on Computer Vision*, pages 4256–4264, 2015.
- [23] Asish Ghoshal and Jean Honorio. Information-theoretic limits of Bayesian network structure learning. In Aarti Singh and Jerry Zhu, editors, *Proceedings of the 20th International Conference on Artificial Intelligence and Statistics*, volume 54 of *Proceedings of Machine Learning Research*, pages 767–775, Fort Lauderdale, FL, USA, 20–22 Apr 2017. PMLR.
- [24] Andrés Gómez and O Prokopyev. A mixed-integer fractional optimization approach to best subset selection. *Optimization-online preprint*, 2018. http://www.optimization-online.org/DB_FILE/2018/09/6795.pdf.
- [25] Sung Won Han, Gong Chen, Myun-Seok Cheon, and Hua Zhong. Estimation of directed acyclic graphs through two-stage adaptive lasso for gene network inference. *Journal of the American Statistical Association*, 111(515):1004–1019, 2016.
- [26] Raymond Hemmecke, Silvia Lindner, and Milan Studený. Characteristic imsets for learning Bayesian network structure. *International Journal of Approximate Reasoning*, 53(9):1336–1349, 2012.
- [27] Mikko Koivisto. Advances in exact bayesian structure discovery in bayesian networks. In *Proceedings of the Twenty-Second Conference on Uncertainty in Artificial Intelligence*, UAI’06, pages 241–248, Arlington, Virginia, USA, 2006. AUAI Press.
- [28] Nevena Lazic, Christopher Bishop, and John Winn. Structural expectation propagation (SEP): Bayesian structure learning for networks with latent variables. In *Artificial Intelligence and Statistics*, pages 379–387, 2013.
- [29] Po-Ling Loh and Peter Bühlmann. High-dimensional learning of linear causal networks via inverse covariance estimation. *Journal of Machine Learning Research*, 15(1):3065–3105, 2014.
- [30] Hasan Manzour, Simge Küçükyavuz, Hao-Hsiang Wu, and Ali Shojaie. Integer programming for learning directed acyclic graphs from continuous data. *Preprint*, 2019. <http://users.iems.northwestern.edu/~simge/Preprints/DAG-Online.pdf>.

- [31] Nicolai Meinshausen and Peter Bühlmann. High-dimensional graphs and variable selection with the lasso. *The Annals of Statistics*, 34(3):1436–1462, 2006.
- [32] Chris. J. Oates, Jim Q. Smith, and Sach Mukherjee. Estimating causal structure using conditional DAG models. *Journal of Machine Learning Research*, 17(54):1–23, 2016.
- [33] Chris J Oates, Jim Q Smith, Sach Mukherjee, and James Cussens. Exact estimation of multiple directed acyclic graphs. *Statistics and Computing*, 26(4):797–811, 2016.
- [34] Temel Öncan, İ Kuban Altinel, and Gilbert Laporte. A comparative analysis of several asymmetric traveling salesman problem formulations. *Computers & Operations Research*, 36(3):637–654, 2009.
- [35] Sascha Ott, Seiya Imoto, and Satoru Miyano. Finding optimal models for small gene networks. In *Pacific Symposium on Biocomputing*, volume 9, pages 557–567. World Scientific, 2004.
- [36] Young Woong Park and Diego Klabjan. Bayesian network learning via topological order. *Journal of Machine Learning Research*, 18(99):1–32, 2017.
- [37] Judea Pearl. Causal inference in statistics: An overview. *Statistics Surveys*, 3:96–146, 2009.
- [38] Jonas Peters and Peter Bühlmann. Identifiability of Gaussian structural equation models with equal error variances. *Biometrika*, 101(1):219–228, 2013.
- [39] Mert Pilanci, Martin J Wainwright, and Laurent El Ghaoui. Sparse learning via Boolean relaxations. *Mathematical Programming*, 151(1):63–87, 2015.
- [40] Garvesh Raskutti and Caroline Uhler. Learning directed acyclic graph models based on sparsest permutations. *Stat*, 7(1):e183, 2018.
- [41] Garvesh Raskutti, Martin J Wainwright, and Bin Yu. Restricted eigenvalue properties for correlated Gaussian designs. *Journal of Machine Learning Research*, 11(Aug):2241–2259, 2010.
- [42] Takumi Saegusa and Ali Shojaie. Joint estimation of precision matrices in heterogeneous populations. *Electronic Journal of Statistics*, 10(1):1341–1392, 2016.
- [43] Ali Shojaie and George Michailidis. Penalized likelihood methods for estimation of sparse high-dimensional directed acyclic graphs. *Biometrika*, 97(3):519–538, 2010.
- [44] Tomi Silander and Petri Myllymäki. A simple approach for finding the globally optimal bayesian network structure. In *Conference on Uncertainty in Artificial Intelligence*, pages 445–452, 2006.
- [45] Liam Solus, Yuhao Wang, Lenka Matejovicova, and Caroline Uhler. Consistency guarantees for permutation-based causal inference algorithms. *arXiv preprint arXiv:1702.03530*, 2017.
- [46] Arjun Sondhi and Ali Shojaie. The reduced pc-algorithm: Improved causal structure learning in large random networks. *Journal of Machine Learning Research*, 20(164):1–31, 2019.
- [47] Peter Spirtes, Clark N Glymour, and Richard Scheines. *Causation, prediction, and search*. MIT press, 2000.

- [48] Milan Studený and David C Haws. On polyhedral approximations of polytopes for learning Bayesian networks. *Journal of Algebraic Statistics*, 4(1), 2013.
- [49] Caroline Uhler, Garvesh Raskutti, Peter Bühlmann, and Bin Yu. Geometry of the faithfulness assumption in causal inference. *The Annals of Statistics*, 41(2):436–463, 2013.
- [50] Sara van de Geer and Peter Bühlmann. ℓ_0 -penalized maximum likelihood for sparse directed acyclic graphs. *The Annals of Statistics*, 41(2):536–567, 2013.
- [51] Linchuan Wei, Andrés Gómez, and Simge Küçükyavuz. On the convexification of constrained quadratic optimization problems with indicator variables. In Daniel Bienstock and Giacomo Zambelli, editors, *Integer Programming and Combinatorial Optimization*, pages 433–447, Cham, 2020. Springer International Publishing.
- [52] Jing Xiang and Seyoung Kim. A* lasso for learning a sparse Bayesian network structure for continuous variables. In *Advances in Neural Information Processing Systems*, pages 2418–2426, 2013.
- [53] Weijun Xie and Xinwei Deng. The CCP selector: Scalable algorithms for sparse ridge regression from chance-constrained programming. *arXiv preprint arXiv:1806.03756*, 2018.
- [54] Cun-Hui Zhang. Nearly unbiased variable selection under minimax concave penalty. *The Annals of Statistics*, 38(2):894–942, 2010.
- [55] Xiaojin Zheng, Xiaoling Sun, and Duan Li. Improving the performance of MIQP solvers for quadratic programs with cardinality and minimum threshold constraints: A semidefinite program approach. *INFORMS Journal on Computing*, 26(4):690–703, 2014.
- [56] Xun Zheng, Bryon Aragam, Pradeep Ravikumar, and Eric P. Xing. Dags with no tears: Continuous optimization for structure learning. In *Proceedings of the 32nd International Conference on Neural Information Processing Systems*, NIPS’18, pages 9492–9503, Red Hook, NY, USA, 2018. Curran Associates Inc.